- What is GPS?
- What is the accuracy of GPS in your phone?
- How do surveyors achieve mm-accuracy GPS measurements?

[last slide of previous lecture]

Dielectric Properties of Materials

Rees discusses 4 categories of materials based on properties of their dielectric constant:

1) non-polar material — ε' and ε'' are constant with ω.
2) polar material (water) — ε' and ε'' vary with ω following the Debye equation.
3) conductive (salt water, copper) $\varepsilon'' = \dfrac{\sigma}{\varepsilon_0 \omega}$
4) plasma (ionosphere) $\varepsilon = n^2 = 1 - \dfrac{Ne^2}{\varepsilon_o m \omega^2}$

   N - electron density

   m - electron mass

   e - electron charge

For a plasma if $n > 0$ the waves travel faster as they travel through the ionosphere. If $n < 0$, n is purely imaginary and all the energy is reflected off the ionosphere. Under typical ionospheric conditions, low-frequency radio waves reflect while higher frequency microwaves can propagate through. Since the ionosphere is dispersive (i.e. speed depends on ω) a dual frequency microwave instrument (a radar altimeter or GPS) can measure the total electron content of a column of ionosphere and can use this to correct for the delay along the path of one or both frequencies.

Ionosphere - Wikipedia

The ionosphere is a shell of electrons and electrically charged atoms and molecules that surrounds the Earth, stretching from a height of about 50 km to more than 1000 km. It owes its existence primarily to ultraviolet radiation from the sun.

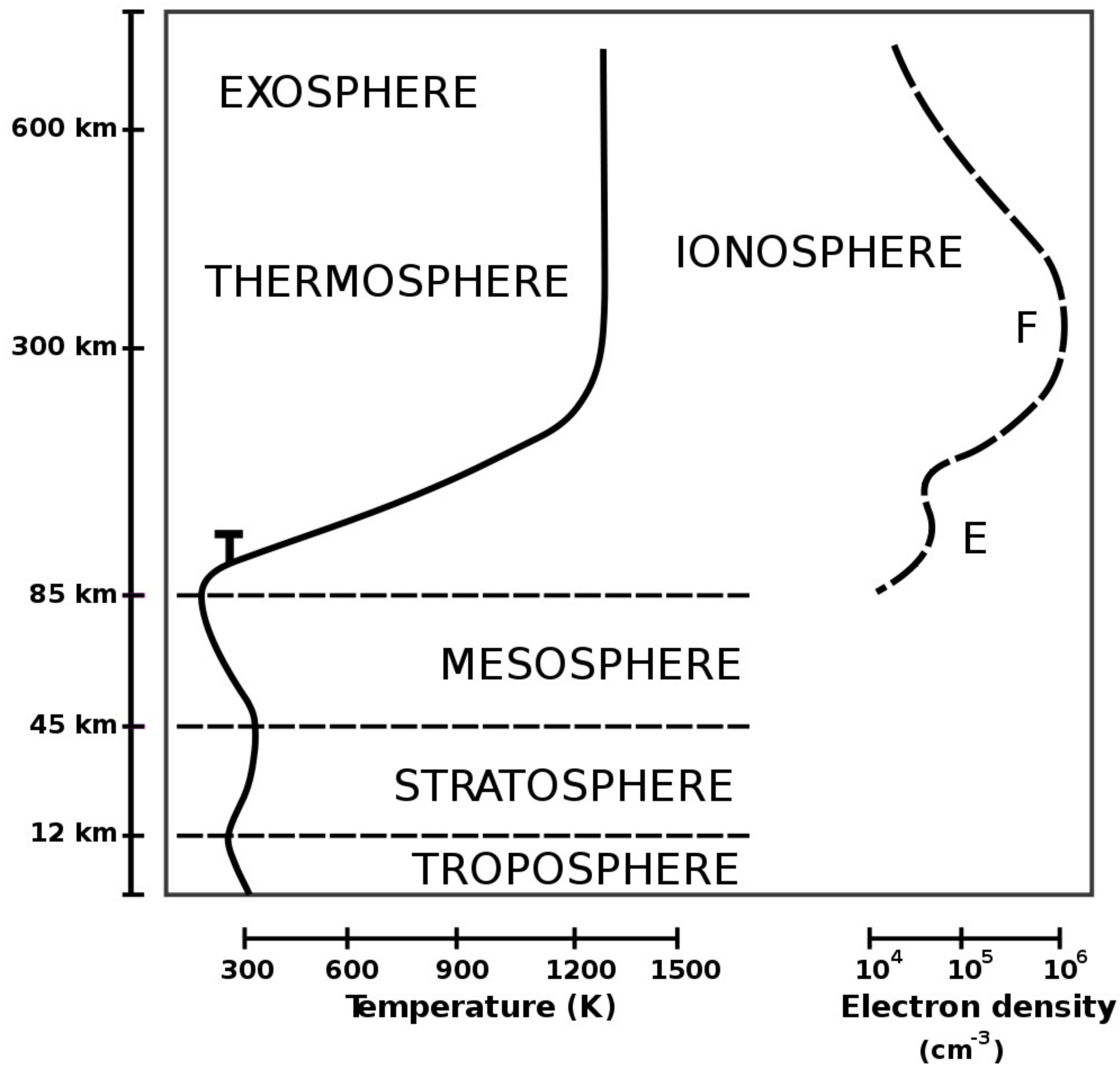

Global Ionospheric Maps (GIM) - JPL

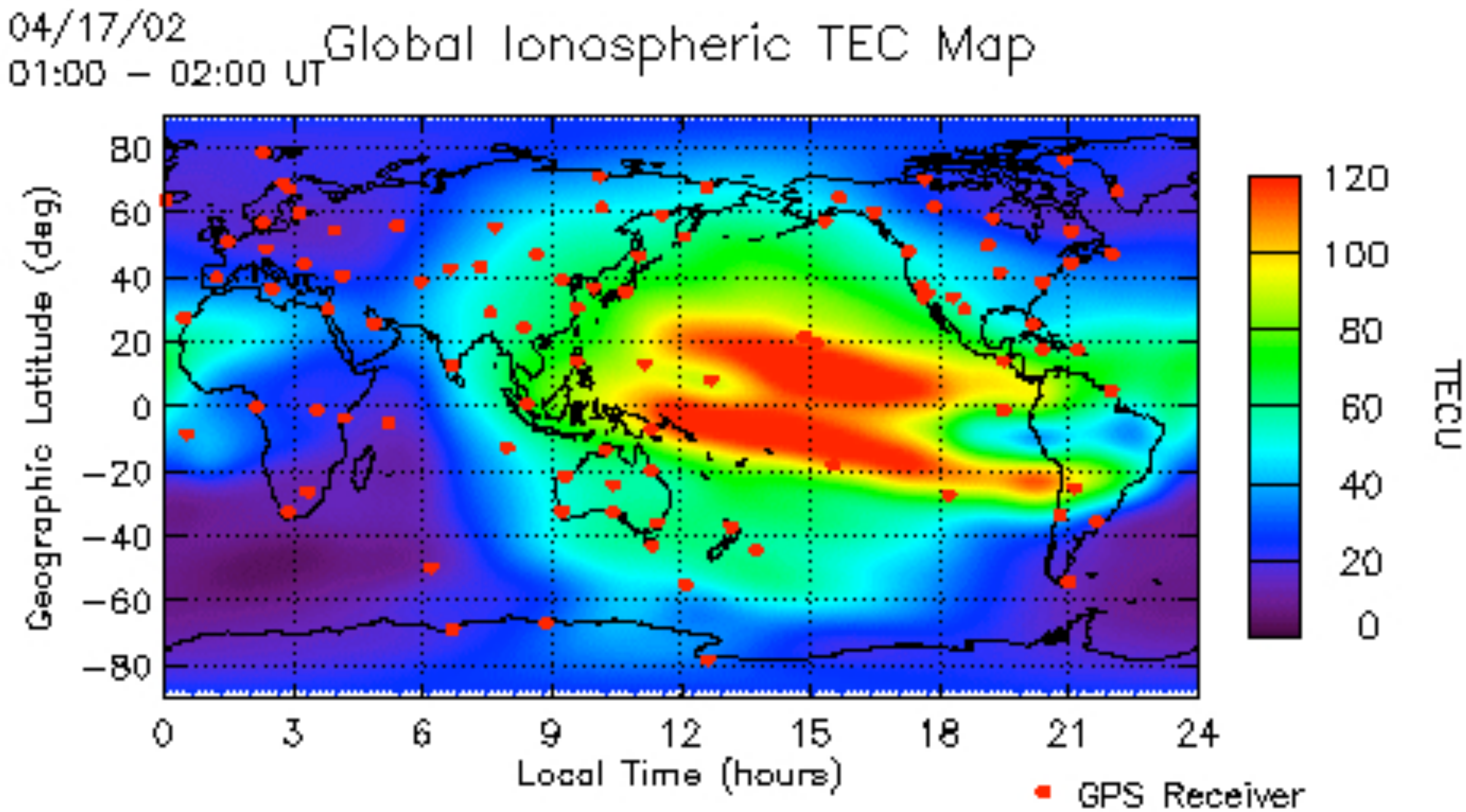

Data from over 100+ continuously operating GPS receivers in a global network are being used to produce global maps of the ionosphere's total electron content (TEC). These Global Ionosphere Maps (GIM) provide instantaneous "snapshots" of the global TEC distribution, by interpolating, in both space and time, the 6-8 simultaneous TEC measurements obtained from each GPS receiver every 30 seconds. The maps can be produced unattended in a real-time mode, with an update rate of 5-15 minutes.

Effects of Ionosphere on Range

index of refraction

$$n = \sqrt{\varepsilon} = \sqrt{1 - \frac{\lambda^2 e^2 N_e}{4\pi^2 m \varepsilon_0 c^2}} \approx 1 - \frac{1}{2}\frac{\lambda^2 e^2 N_e}{4\pi^2 m \varepsilon_0 c^2} = 1 - K\lambda^2 N_e$$

N_e - electron density
e - electron charge
m - electron mass
λ - radar wavelength
c - speed of light
ε_o - permittivity of free space

phase velocity > c

$$v_p = c / n$$

vertical travel time change

$$\Delta\tau = \int_0^H (1/v_p - 1/c)\,dz = -\frac{K\lambda^2}{c}\int_0^H N_e(z)\,dz = -\frac{K\lambda^2}{c} TEC$$

range change

$$\Delta\rho = -K\lambda^2 TEC$$

L-band example
(1-way vertical)

$$\Delta\rho = -25cm * \text{TECU}$$

CGPS Coverage

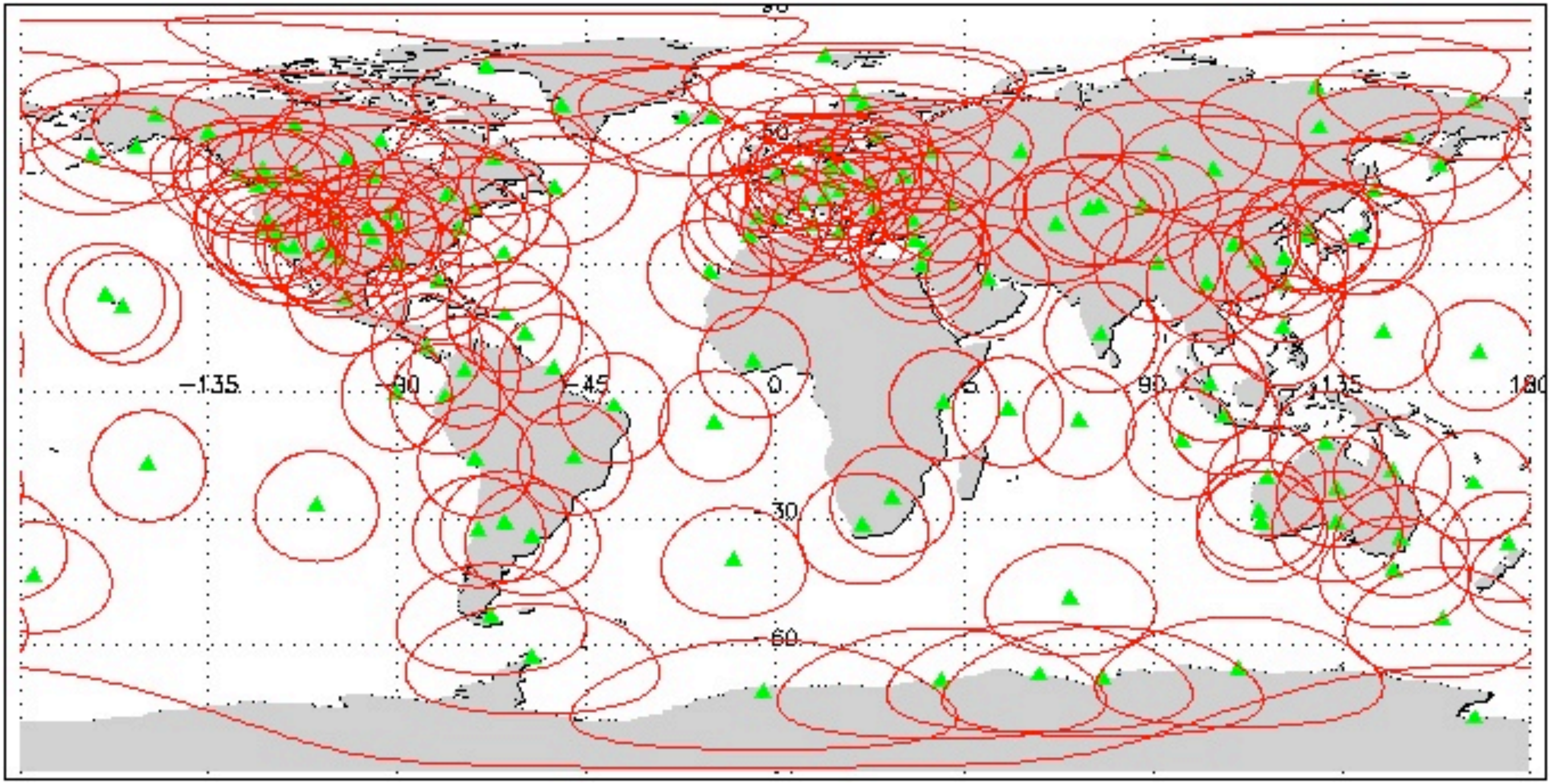

Data from over 100+ continuously operating GPS receivers in a global network are being used to produce global maps of the ionosphere's total electron content (TEC). These Global Ionosphere Maps (GIM) provide instantaneous "snapshots" of the global TEC distribution, by interpolating, in both space and time, the 6-8 simultaneous TEC measurements obtained from each GPS receiver every 30 seconds. The maps can be produced unattended in a real-time mode, with an update rate of 5-15 minutes.

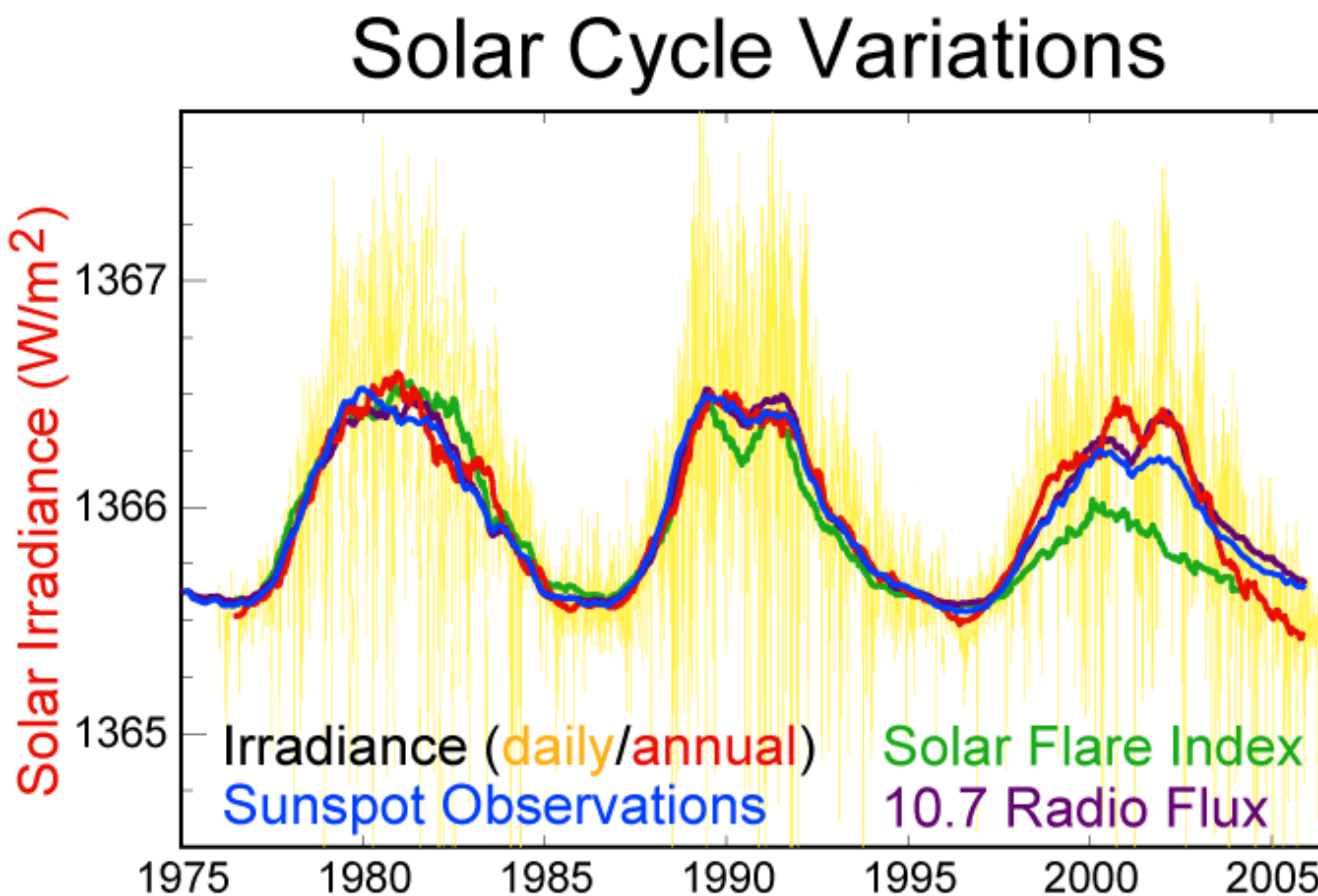

Activity cycles 21, 22 and 23 seen in sunspot number index, TSI, 10.7cm radio flux, and flare index. The vertical scales for each quantity have been adjusted to permit overplotting on the same vertical axis as TSI. Temporal variations of all quantities are tightly locked in phase, but the degree of correlation in amplitudes is variable to some degree. [Wikipedia]

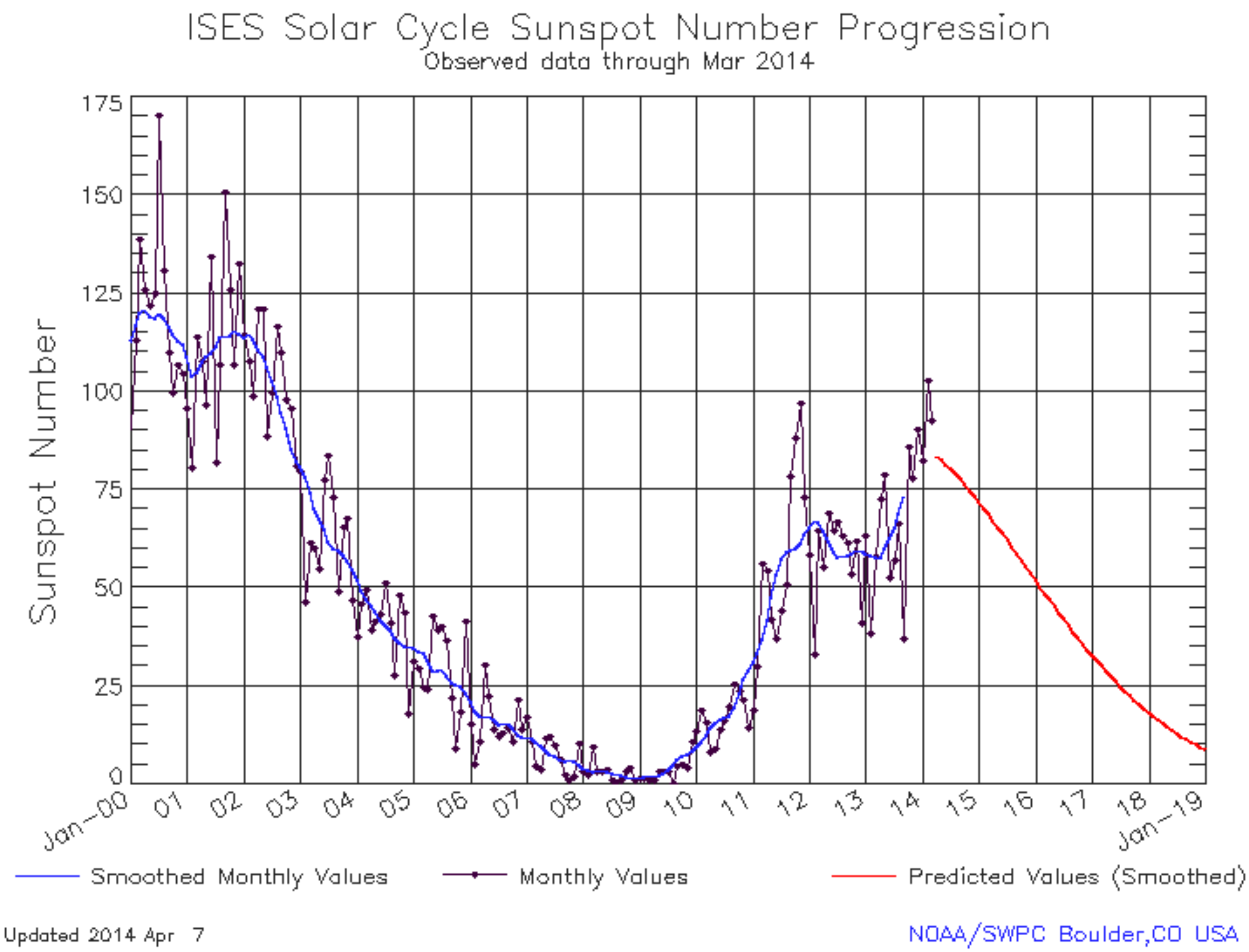

May 8, 2009 -- The Solar Cycle 24 Prediction Panel has reached a consensus decision on the prediction of the next solar cycle (Cycle 24). First, the panel has agreed that solar minimum occurred in December, 2008. This still qualifies as a prediction since the smoothed sunspot number is only valid through September, 2008. The panel has decided that the next solar cycle will be below average in intensity, with a maximum sunspot number of 90. Given the predicted date of solar minimum and the predicted maximum intensity, solar maximum is now expected to occur in May, 2013. Note, this is a consensus opinion, not a unanimous decision. A supermajority of the panel did agree to this prediction. [http://www.swpc.noaa.gov/SolarCycle/]

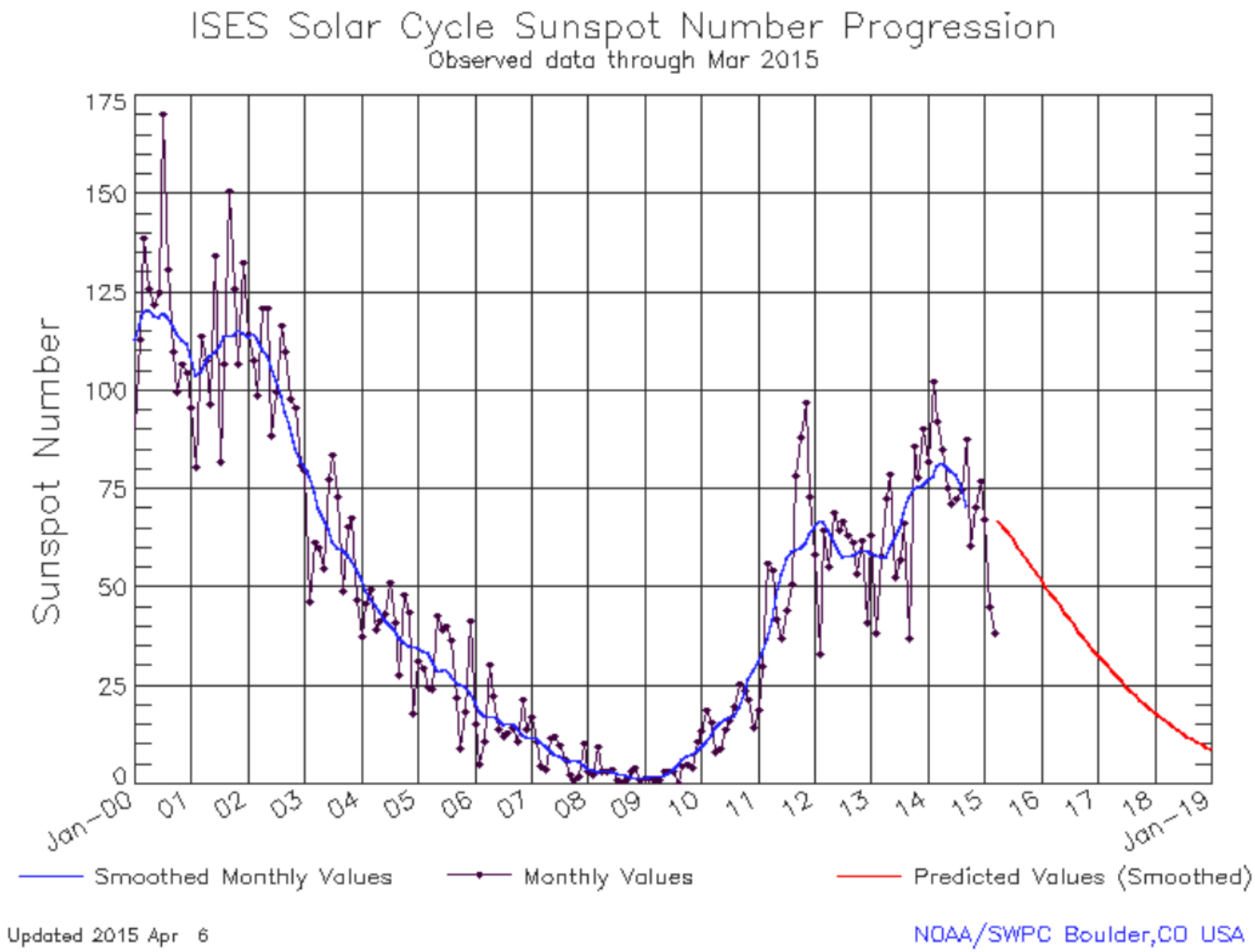

May 8, 2009 -- The Solar Cycle 24 Prediction Panel has reached a consensus decision on the prediction of the next solar cycle (Cycle 24). First, the panel has agreed that solar minimum occurred in December, 2008. This still qualifies as a prediction since the smoothed sunspot number is only valid through September, 2008. The panel has decided that the next solar cycle will be below average in intensity, with a maximum sunspot number of 90. Given the predicted date of solar minimum and the predicted maximum intensity, solar maximum is now expected to occur in May, 2013. Note, this is a consensus opinion, not a unanimous decision. A supermajority of the panel did agree to this prediction. [http://www.swpc.noaa.gov/SolarCycle/]

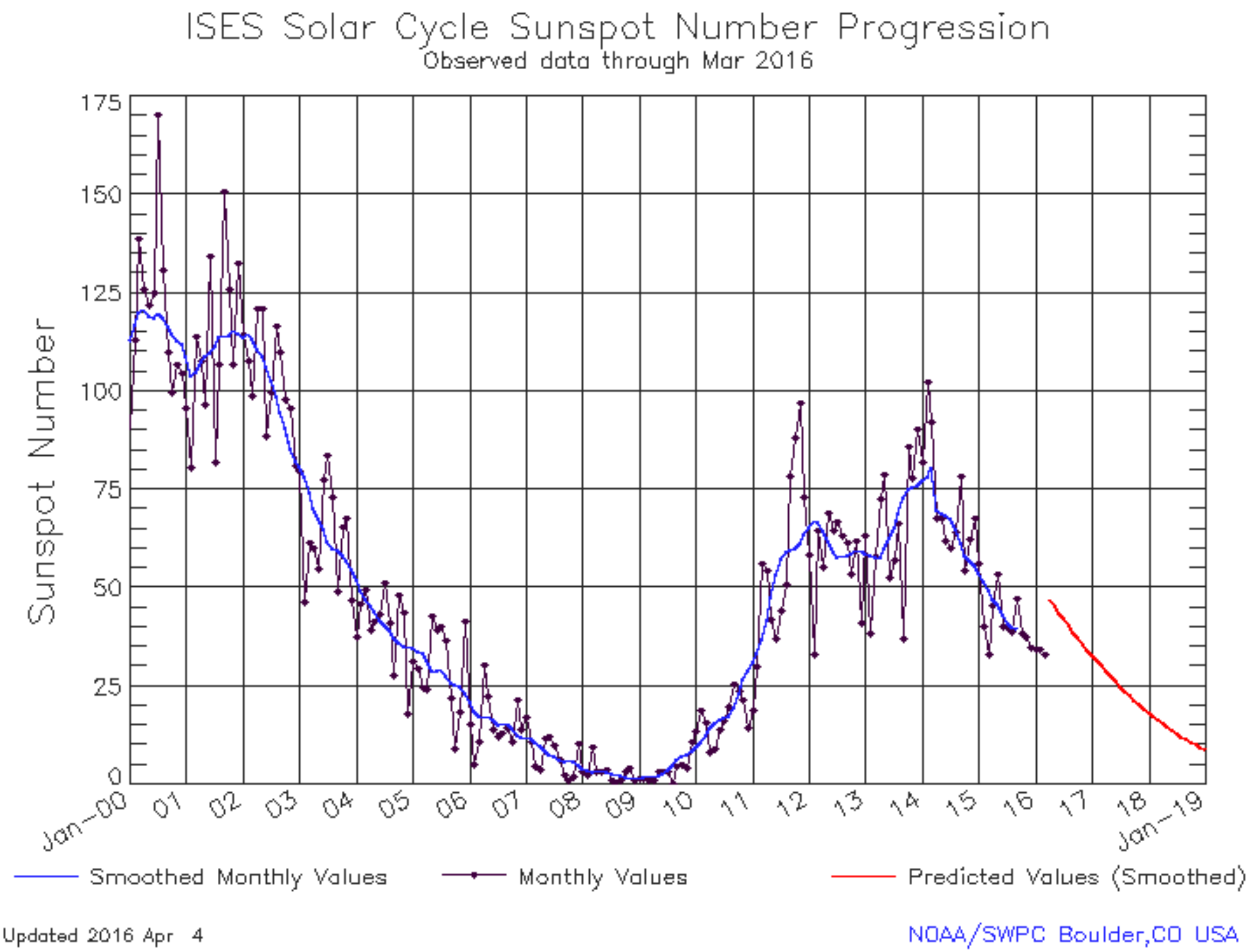

May 8, 2009 -- The Solar Cycle 24 Prediction Panel has reached a consensus decision on the prediction of the next solar cycle (Cycle 24). First, the panel has agreed that solar minimum occurred in December, 2008. This still qualifies as a prediction since the smoothed sunspot number is only valid through September, 2008. The panel has decided that the next solar cycle will be below average in intensity, with a maximum sunspot number of 90. Given the predicted date of solar minimum and the predicted maximum intensity, solar maximum is now expected to occur in May, 2013. Note, this is a consensus opinion, not a unanimous decision. A supermajority of the panel did agree to this prediction. [http://www.swpc.noaa.gov/SolarCycle/]

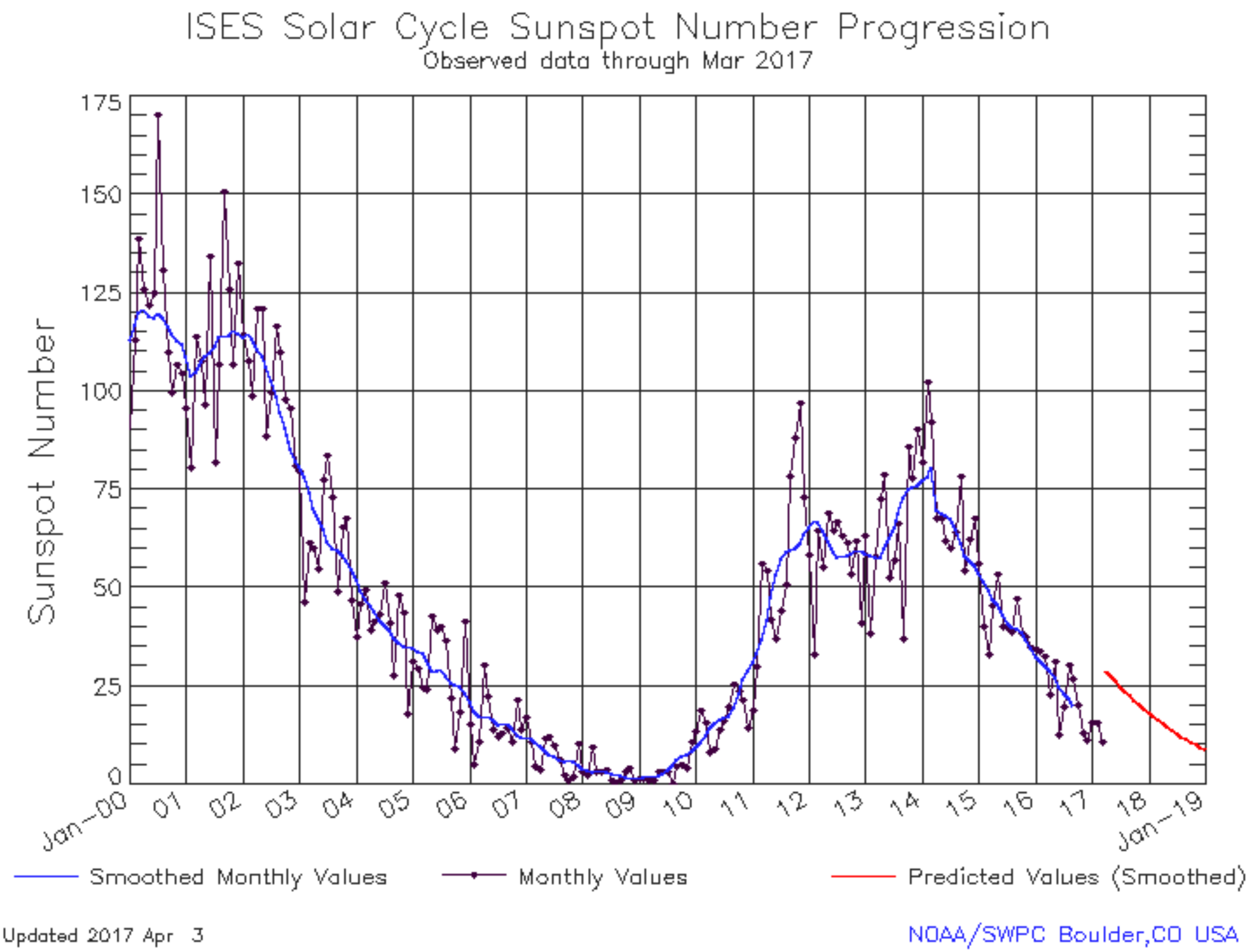

May 8, 2009 -- The Solar Cycle 24 Prediction Panel has reached a consensus decision on the prediction of the next solar cycle (Cycle 24). First, the panel has agreed that solar minimum occurred in December, 2008. This still qualifies as a prediction since the smoothed sunspot number is only valid through September, 2008. The panel has decided that the next solar cycle will be below average in intensity, with a maximum sunspot number of 90. Given the predicted date of solar minimum and the predicted maximum intensity, solar maximum is now expected to occur in May, 2013. Note, this is a consensus opinion, not a unanimous decision. A supermajority of the panel did agree to this prediction. [http://www.swpc.noaa.gov/SolarCycle/]

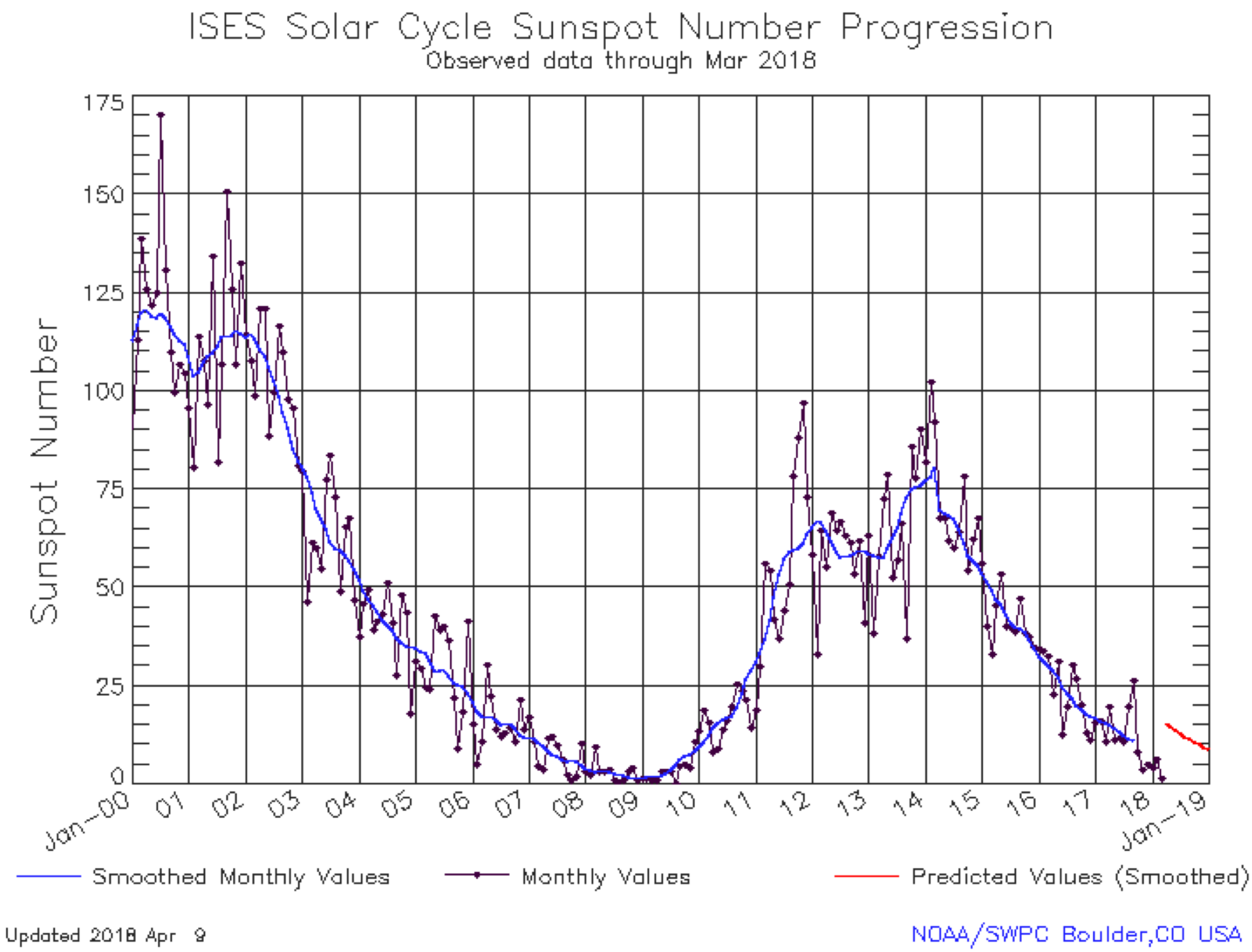

May 8, 2009 -- The Solar Cycle 24 Prediction Panel has reached a consensus decision on the prediction of the next solar cycle (Cycle 24). First, the panel has agreed that solar minimum occurred in December, 2008. This still qualifies as a prediction since the smoothed sunspot number is only valid through September, 2008. The panel has decided that the next solar cycle will be below average in intensity, with a maximum sunspot number of 90. Given the predicted date of solar minimum and the predicted maximum intensity, solar maximum is now expected to occur in May, 2013. Note, this is a consensus opinion, not a unanimous decision. A supermajority of the panel did agree to this prediction. [http://www.swpc.noaa.gov/SolarCycle/]

Effects of Solar Cycle on Remote Sensing Satellites

- path errors in GPS, radar altimetry, and InSAR

  phase velocity > *c*

  group velocity < *c*

  error proportional to wavelength squared

  Ku 23 mm - 0.1 m delay

  C 56 mm - 0.8 m

  L 150 mm - 5.0 m delay

- increased atmospheric drag on low orbiting satellites (e.g. GRACE - 400 km, GOCE - 250 km)

- risk to spacecraft health during solar maximum (South Atlantic anomaly)

Effects of Ionosphere on Range

index of refraction

$$n = \sqrt{\varepsilon} = \sqrt{1 - \frac{\lambda^2 e^2 N_e}{4\pi^2 m \varepsilon_0 c^2}} \approx 1 - \frac{1}{2}\frac{\lambda^2 e^2 N_e}{4\pi^2 m \varepsilon_0 c^2} = 1 - K\lambda^2 N_e$$

N_e - electron density
e - electron charge
m - electron mass
λ - radar wavelength
c - speed of light
ε_o - permittivity of free space

phase velocity > c

$$v_p = c / n$$

vertical travel time change

$$\Delta\tau = \int_0^H (1/v_p - 1/c)\,dz = -\frac{K\lambda^2}{c}\int_0^H N_e(z)\,dz = -\frac{K\lambda^2}{c} TEC$$

range change

$$\Delta\rho = -K\lambda^2 TEC$$

L-band example
(1-way vertical)

$$\Delta\rho = -25cm * \mathrm{TECU}$$

Ionospheric phase ramps and waves are evident in co-seismic interferometry of Wenchuan earthquake.

Waves also cause azimuth shifts resulting in wave-like areas of lower coherence.

Can global ionospheric models be used to correct the ramps?

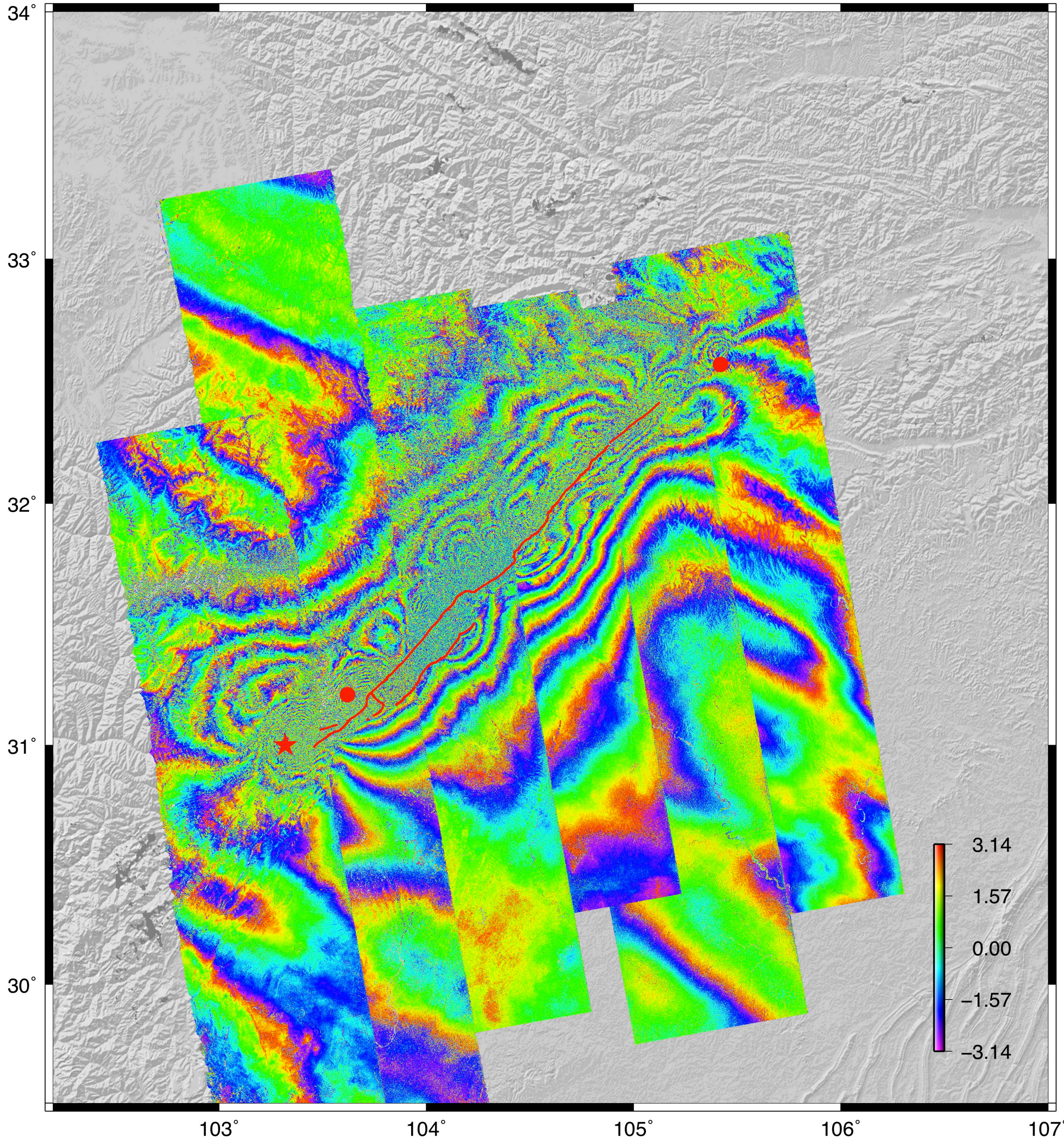

[Tong et al., revised for JGR, 2009]

Residual phase for ALOS interferometry over Japan.

Ascending tracks 10:30 PM

11.8 cm/cycle

Waves and ramps are probably due to ionospheric phase advance.

[Shimada et al., DPRI Workshop, Kyoto September 2009]

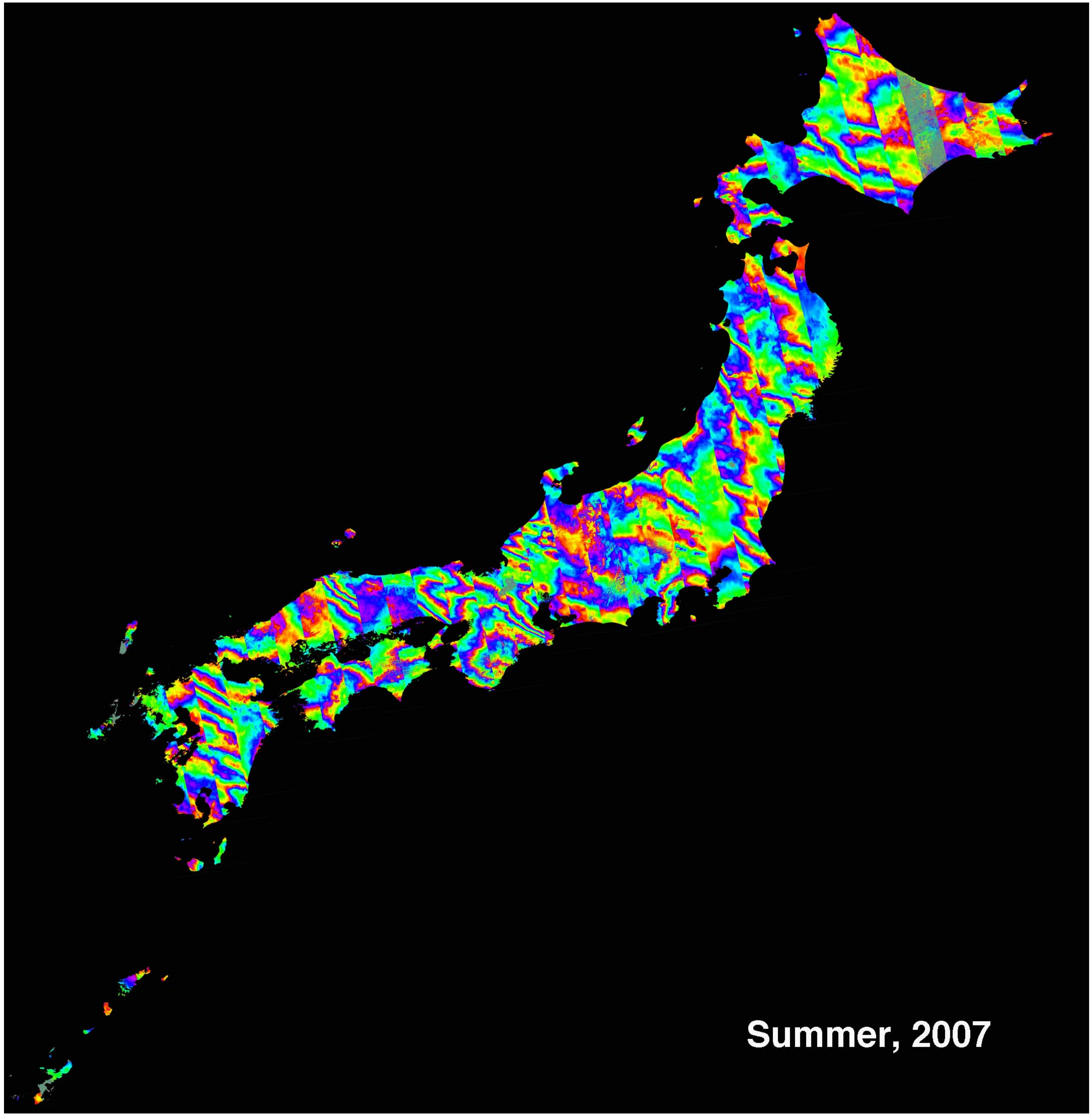

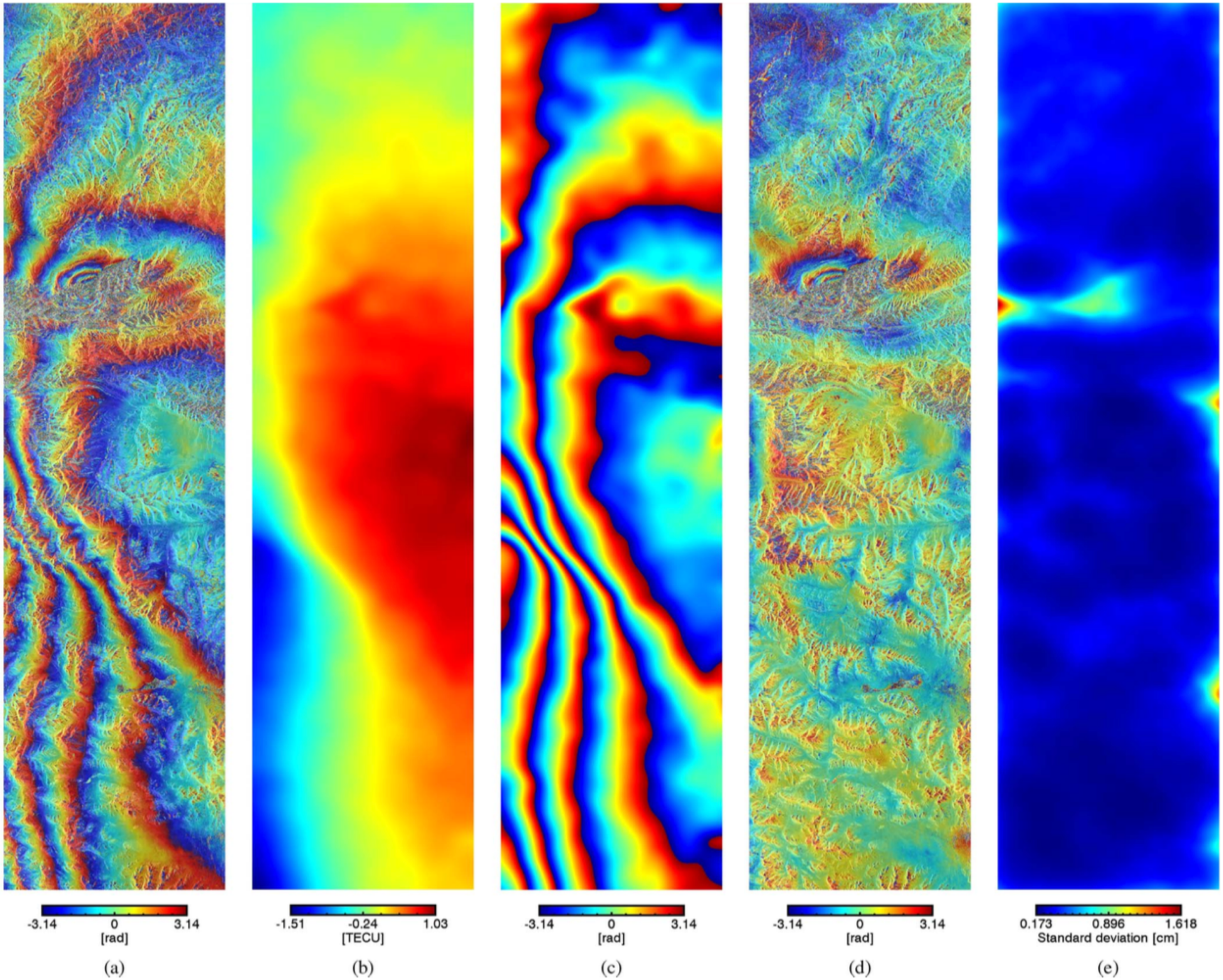

Fig. 5. (a) Kyrgyzstan 2008 earthquake of October 5 can be recognized in the top part of the interferogram. Five fringes in the bottom part of (a) are supposed to be due to ionosphere changes. (b) The ionospheric TEC map, estimated using the split-spectrum method, converted to a (c) phase screen, is used to produce the (d) ionosphere-compensated interferogram. (e) Expected accuracy of the ionosphere estimation. Azimuth length is 283 km; range length is 68 km.